Effect of Na_2SO_4 Coating layer on Nickel-Rich $Li(Ni_xCo_yMn_z)O_2$ Cathode Materials for Lithium-Ion Batteries

*Jaewon Choi, Jinwoo Kim, Kyu-Tae Lee, Jaehong Lim, Jaeho Lee, and Young Soo Yun**

Lithium-ion batteries (LIBs) have attracted considerable attention as a sustainable energy storage system because of their high energy density, low cost, and long cycle life.[1] The range of applications of LIBs has increased from small, high-technology devices (e.g., mobile phones, tablets, laptops, etc.) to large-scale devices (e.g., electric vehicles) and energy-storage systems (ESS).[2] On the other hand, commercial lithium-ion batteries still require improvements in their electrochemical performance, such as higher capacity, working voltage, and cyclic performance to be applicable to large-scale battery systems. Several attempts have been made to obtain high energy density cathode materials for lithium-rich layered oxide materials (Li_2MnO_3-$LiMO_2$, M = Mn, Li, Co, Fe, Cr, etc.), $LiCoO_2$, spinel $LiMn_2O_4$, olivine $LiFePO_4$, etc.[3]

Ni-rich ($x \geq 0.5$, $x + y + z = 1$) layered $Li(Ni_xCo_yM_z)O_2$ (M = Mn, Al) has become one of the most promising candidates for cathode materials in high performance LIBs. The high proportion of Ni contributes to the advancement of the specific capacity and ensures low production costs.[4] Despite these advantages, the poor cycle life of Ni-rich layered $Li(Ni_xCo_yM_z)O_2$ is a critical problem because the layered $LiNiO_2$ structure commonly suffers from structural degradation, the accumulation of a thick solid electrolyte interface (SEI) layer and the damage induced from the acidic chemicals (HF, HCl, etc.) during cycling.[5] To prevent the most common side reactions, such as the high degree of de-lithiation and decomposition of the surface of the cathode materials, a range of materials, such as metal oxides (Al_2O_3, SiO_2, ZnO), phosphates ($AlPO_4$), fluorides (LiF), polymers, and carbon, have been employed to coat the surface of the layered $LiNiO_2$, resulting in an improved cycling stability of Ni-rich $Li(Ni_xCo_yM_z)O_2$.[6] Among them, continuous surface coating methods have been proven to be the best strategy to improve the electrochemical performance.[7]

Prof. Y. S. Yun
Department of Chemical Engineering
Kangwon National University
Samcheok 245–711, Korea
E-mail: ysyun@kangwon.ac.kr
Dr. J. Choi, Dr. J. Kim, Dr. K. Lee
Department of Materials Science and Engineering
University of Illinois at Urbana-Champaign
Urbana, Illinois 61801, USA
Dr. J. Choi, Dr. J. Lim, J. Lee
Corporate R&D Center
Samsung SDI Co. Ltd., Yongin, Gyunggido 446–577, Korea

DOI: 10.1002/admi.201600784

This paper reports the synthesis of continuous Na_2SO_4-coated Ni-rich $LiNi_{0.88}Co_{0.10}Mn_{0.02}O_2$ (S-NCM8) by sodium dodecyl sulfate (SDS). S-NCM8 showed an improved cyclic performance in LIBs, compared to the washed $LiNi_{0.88}Co_{0.10}Mn_{0.02}O_2$ (W-NCM8) and bare $LiNi_{0.88}Co_{0.10}Mn_{0.02}O_2$ (B-NCM8). As a result, a continuous Na_2SO_4 coating layer of S-NCM8 prevents direct contact between the active surface of the Ni-rich $Li(Ni_xCo_yMn_z)O_2$ and the electrolyte. In addition, the coating layer improved the conductivity and reduced the resistance on the surface of S-NCM8. The effects of Na_2SO_4 coating layers were demonstrated further using commercial bare $LiNi_{0.5}Co_{0.2}Mn_{0.3}O_2$ (B-NCM5, Ecopro Co.) powder.

Figure 1 presents the key steps of the synthesis of Na_2SO_4-coated Ni-rich $Li(Ni_xCo_yMn_z)O_2$. In the synthesis of $LiNi_{0.88}Co_{0.10}Mn_{0.02}O_2$ (NCM8) (Figure 1a), the coprecipitate $(Ni_{0.9}Co_{0.1})OH_2$ precursors were mixed with $LiOH \cdot H_2O$ and manganese oxide using a mechanical mixer.[8] The Li/transition metal molar ratio of each mixture was fixed to 1.02 (excess Li source) to prepare the lithium composite metal oxide with a large nickel content. As a result, from the residual lithium source, unwanted Li_2CO_3 and LiOH formed on the surface of NCM8 after annealing for 10 h at 750 °C. As shown in Figure 1b, NCM8 was washed in deionized water for 20 min to remove any residual Li_2CO_3 and LiOH, because these can cause problems for the LIB performance, such as structural degradation of the cathode material, gas emission during electrochemical cycling, and electrode slurry gelation (Figure S1, Supporting Information). In the following step, the cleaned NCM8 (100 g) was dissolved in DI water (95 mL), and SDS (1 g, 1 wt.%) was added to the solution. The reaction mixture was then heated to 120 °C for 2 h (Figure 1c). The same procedure was applied to obtain B-NCM5 to demonstrate the effects of the Na_2SO_4 coating layers in a commercial cathode system. Because SDS is composed of both a hydrophobic aliphatic hydrocarbon group and a hydrophilic sulfate group, it can form a micelle structure-like coating layer on the surface of the NCM materials in aqueous solution.[9] Whereas the hydrophobic moiety of SDS could be adsorbed on the surface of the NCM materials, its hydrophilic block could be heading for the aqueous solution, as shown in Figure 1c. As a final step, the resulting SDS-coated NCM materials were annealed at 750 °C for 5 h in O_2 atmosphere to remove the aliphatic carbon chain of SDS, any residual water, and impurities. Eventually, continuous Na_2SO_4-coated NCM materials were prepared (Figure 1d).

Figure 2a–f presents the morphologies of the resulting materials obtained through the above coating process characterized by high- and low-magnification scanning electron

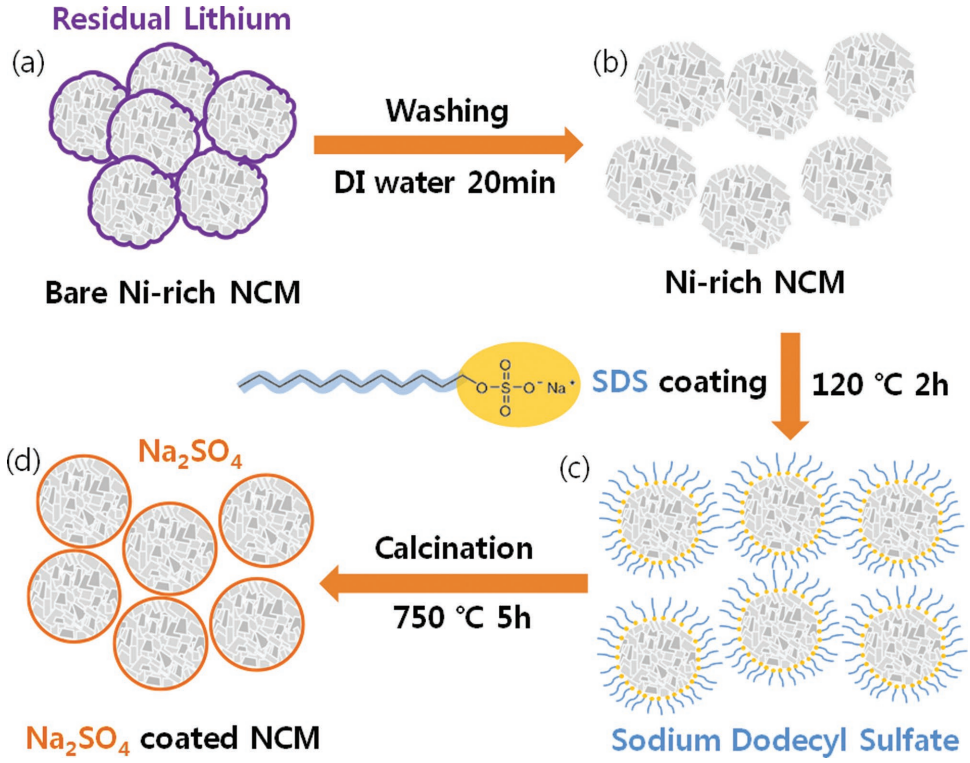

Figure 1. Key steps for the synthesis of Na_2SO_4-coated Ni-rich $Li(Ni_xCo_yMn_z)O_2$: a) Bare NCM, b) washed NCM, c) SDS powd er coating on the surface of NCM, and d) resulting Na_2SO_4-coated NCM.

microscopy (SEM): a,b) B-NCM8, c,d) W-NCM8, e,f) S-NCM8, g,h) B-NCM5, and i,j) SDS-coated NCM5. Both B-NCM8 and B-NCM5 have a bimodal distribution of a spherical outline of about 3 and 10 µm in diameter, respectively (Figure 2a,b,g,h). After SDS coating, no distinct morphology or volume changes were observed compared to the bare and washed NCM materials (Figure 2e,f,i,j). As shown in the digital photographs, Figure 2k and l, the commercial Na_2SO_4-coated electrode slurry has a white color, whereas the SDS-coated NCM8 showed a conventional black slurry without any floating matter, suggesting that the Na_2SO_4 is not well-coated on the surface of the NCMs. Therefore, coating with SDS followed by calcination can be an alternative method for producing a homogeneous coating of Na_2SO_4 layers on the surface of NCMs.

Figure 3a shows the X-ray diffraction (XRD) patterns of S-NCM8, S-NCM5, and heat-treated SDS powder at 750 °C for 5 h in O_2 atmosphere. In the heat-treated SDS, the SDS was transformed to Na_2SO_4 (black line). The XRD patterns of S-NCM8 (red line) and S-NCM5 (blue line) were in accordance with the hexagonal α-$NaFeO_2$ layered structure belonging to the *R*3*m* space group.[10] No obvious impurity peaks could be discerned. In addition, the absence of any Na_2SO_4 peaks could be explained by the fact that the SDS coating layer was only very thin. On the other hand, as shown in Figure 3b,c the energy-dispersive X-ray spectroscopy (EDS) mapping images of S-NCM8 and S-NCM5 showed a homogeneous distribution of sodium and sulfur on their surfaces.

An Auger depth profile analysis for the chemical component of sulfur was carried out to determine the Na_2SO_4 coating on the surface of the NCMs, as shown in Figure 3d. The quantitative sulfur depth profile of S-NCM8 showed a large intensity (ca. 1.1%) at a depth of around 10 nm compared to those of W-NCM8 and B-NCM8, indicating that Na_2SO_4 layers of around 10 nm are coated on the surface of S-NCM8. In addition, inductively coupled plasma – atomic emission spectroscopy (ICP-AES) showed that the sodium to sulfur weight ratio increased with increasing SDS quantity added to the synthesis process (Figure S2, Supporting Information). Further investigation of the surface chemical states of the coating layer by X-ray photoelectron spectroscopy (XPS) is shown in Figure 3e. The S 2p spectra of W-NCM8 and B-NCM8 showed distinct peaks centered at around 168.8 eV.[11] In addition, the S 2p spectrum of S-NCM8 showed a similar peak with a stronger intensity. This peak originated from the Na-S bonding in Na_2SO_4,[12] supporting that the Na_2SO_4 coating layer was introduced onto the surface of S-NCM8.

Galvanostatic charge/discharge tests of the cathode materials using S-NCM8, W-NCM8, B-NCM8, B-NCM5, and S-NCM5 (2032 type coin cells) were performed, as shown in **Figure 4**. The coin cells were cycled between 2.8 V and 4.3 V at different current densities (the 1 C-rate of NCM8 and W-NCM8 was 190 mAg^{-1} and 150 mAg^{-1}, respectively) from a 0.1 to 5 C-rate and recovered from a 5 to a 1 C-rate (Figure 4a). All cells lost their discharge capacity gradually with increasing C-rate, and S-NCM8 showed a higher capacity in the overall C-rate range compared to all other samples. For S-NCM8, an 18.4% loss of discharge capacity was exhibited at the 5 C rate, whereas B-NCM8 showed a 21.8% loss of discharge capacity at the same current rate. Moreover, after 100 cycles, S-NCM8 showed a more stable capacity retention of 85.2% compared to 65.2% and 80.3%

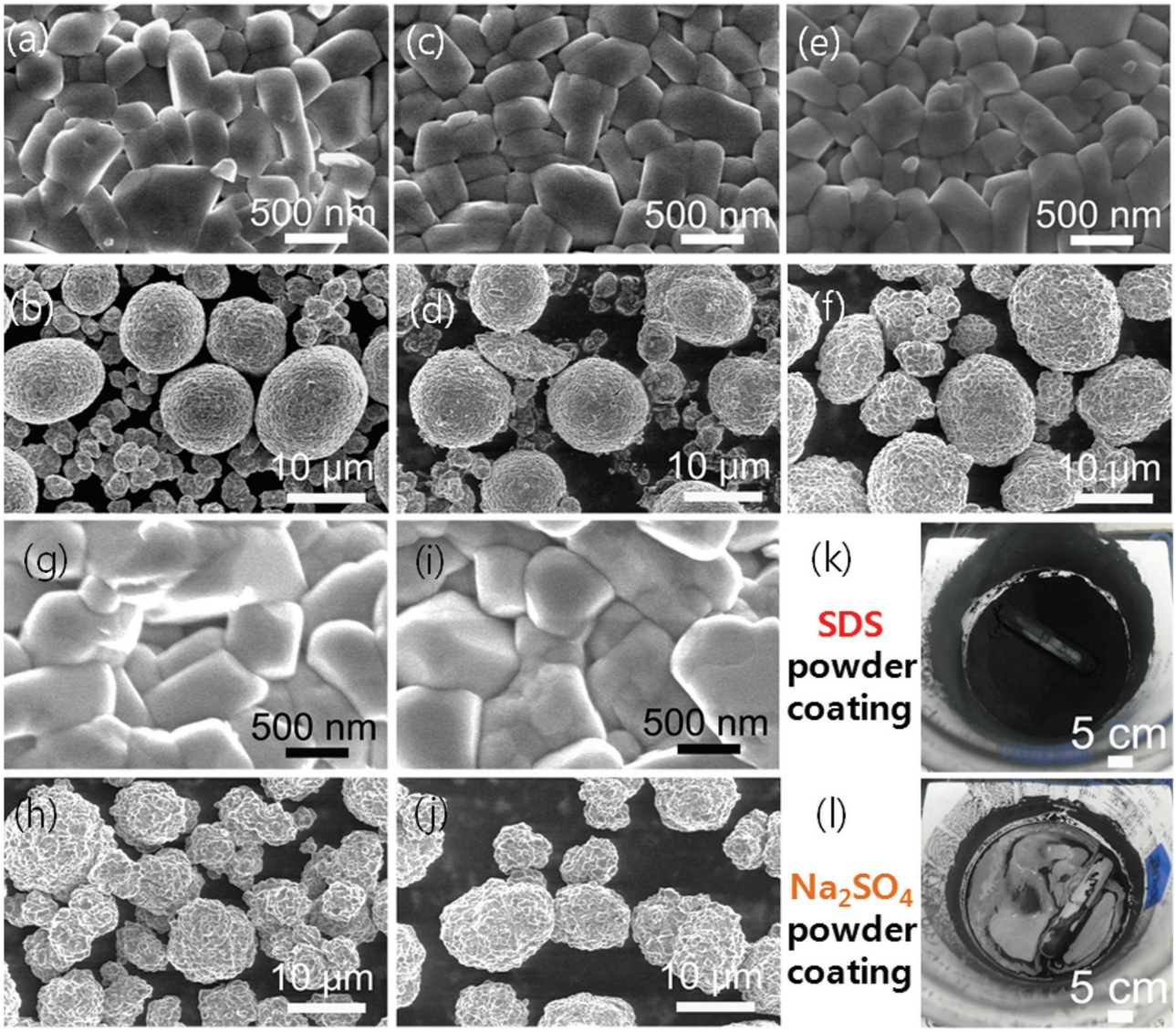

Figure 2. SEM images of high- and low-magnification of: a,b) B-NCM8, c,d) W-NCM8, e,f) S-NCM8, g,h) B-NCM5, and i,j) S-NCM5. k,l) Digital photograph of SDS-coated NCM8 (k) and commercial Na_2SO_4-coated NCM8 (l).

of W-NCM8 and B-NCM8, respectively (Figure 4b). For the large battery test with a commercial graphite anode in 18650 type cells, the S-NCM8-based battery showed not only an enhanced cycle retention of 96.1% (W-NCM8, 95.7%), but also a more stable cycle performance compared to W-NCM8 (Figure S3, Supporting Information). Rate capability and cyclic tests of S-NCM8 prepared with various amount of SDS were also carried out (Figure S4, Supporting Information), which shows that S-NCM8 prepared with 1 wt% SDS exhibited the best performance both in terms of rate capability and cyclic performance. For S-NCM5, a similar enhancement in rate capability was observed, compared to B-NCM5 (Figure 4c). On the other hand, S-NCM5 showed an enhanced cycle retention compared to that of B-NCM5 (Figure 4d).

The conductivities and resistances of S-NCM8 and W-NCM8 were characterized, as shown in Figure 4e,f. At a pressure of 20 kN, S-NCM8 showed a significantly higher conductivity (ca. 2.6 times) and lower resistance (ca. 2.7 times) than W-NCM8, respectively. These superior electrical properties of S-NCM8 provide a more detailed understanding of improvements in the rate capability and cycle performance.[13] The outstanding electrochemical stability as well as the conductivity and low resistance of S-NCM8 can be attributed to the Na_2SO_4 coating layers on the surface of NCMs.

In conclusion, Na_2SO_4-coated nickel-rich NCM materials were prepared by SDS coating followed by calcination. S-NCM8 showed an enhanced rate capability because Na_2SO_4-coating layers improve their conductivity significantly and reduce their resistance. In addition, S-NCM8 showed a greater cycle stability than B-NCM8 because the Na_2SO_4-coating layers effectively mitigate nickel dissolution during the cycling test. Similar results were obtained when performing the same experiment using commercial NCMs with a Na_2SO_4 coating layer. These Na_2SO_4 coating layers fabricated from SDS have great potential as

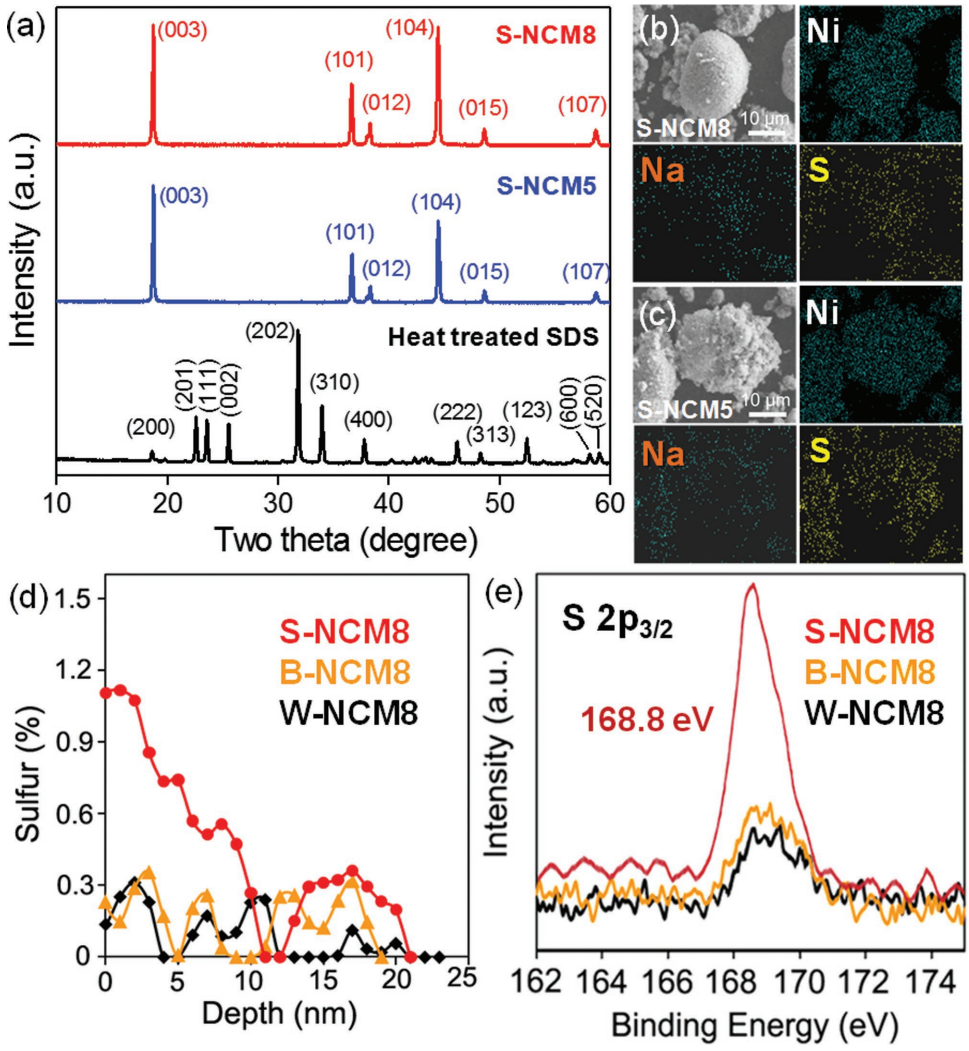

Figure 3. a) Powder X-ray diffraction patterns of S-NCM8, S-NCM5, and heat-treated SDS powder. b,c) SEM and EDS-mapping images (Ni, Na, and S) of S-NCM8 (b) and S-NCM5 (c). d) Auger depth profiles showing the atomic content of sulfur in S-NCM8, W-NCM8, and B-NCM8. e) Sulfur $2p_{3/2}$ orbital peaks in the XPS spectra of S-NCM8, W-NCM8, and B-NCM8 materials.

surface coating materials on nickel-rich NCM materials for LIBs.

Experimental Section

Materials and Procedure: The hydroxide precursor $(Ni_{0.9}Co_{0.1})OH_2$ was prepared by a coprecipitation method.[11] For the synthesis of NCM8, $(Ni_{0.9}Co_{0.1})OH_2$ precursors (100 g), lithium hydroxide ($LiOH\text{-}H_2O$, Samchun Chemicals, 47.10 g) and manganese oxide (MnO_2, Sigma Aldrich, 1.91 g) were added to a mechanical mixer and mixed thoroughly for 30 min. The Li/TM(lithium/transition metal) molar ratio was fixed to 1.02 for all samples. The mixed samples were calcined at 750 °C for 10 h in O_2 atmosphere to form the samples. The heating and cooling rates for the samples were 5 °C min^{-1}. To prepare W-NCM8, 100 g of each sample was dispersed in 100 mL of deionized water. The solution was mixed thoroughly for 10 min, and dried at 120 °C for 5 h. For the Na_2SO_4 coating from SDS the NCM materials (100 g), such as NCM8 and NCM5 (Ecopro Co. materials), were dispersed in deionized water (95 mL) at room temperature for 1 h. The Na_2SO_4 coating solution was prepared by dissolving sodium dodecyl sulfate (Aldrich, 1 g, 1 wt%) in deionized water (5 mL). After 1 h, the SDS solution was added to the NCM material solution. Subsequently the solution was heated to 120 °C for 2 h. The resulting powder was annealed at 750 °C for 5 h in O_2 atmosphere.

Electrochemical Testing: NCM cathode materials (10 g), carbon black (1 g), and polyvinylidene fluoride binder (2 g) were mixed with *N*-methylpyrrolidone (NMP, 5 g). After coating the aluminum foil with this slurry, the electrode was dried under vacuum at 110 °C overnight. The diameter of the circular aluminum electrode was 14 mm. The loading level of the electrode materials was 10 mg cm^{-2}. The cell tests were conducted using coin-type half cells (CR 2032) with lithium metal as the counter electrode and 1.3 M $LiPF_6$ in ethylene carbonate/ethyl methyl carbonate:dimethyl carbonate (EC/EMC/DMC = 3:4:3, v/v/v) as the electrolyte. The discharge/charge cycle tests were performed using an automatic battery cycling system.

Characterization: Low- and high-resolution scanning electron microscopy (SEM) were performed using a Philips XL30 in secondary electron mode. Energy-dispersive spectroscopy (EDS) was obtained in field-emission mode. Powder X-ray diffraction (XRD) patterns were taken using a Rigaku D-max 2500 and filtered Cu Kα radiation. Depth

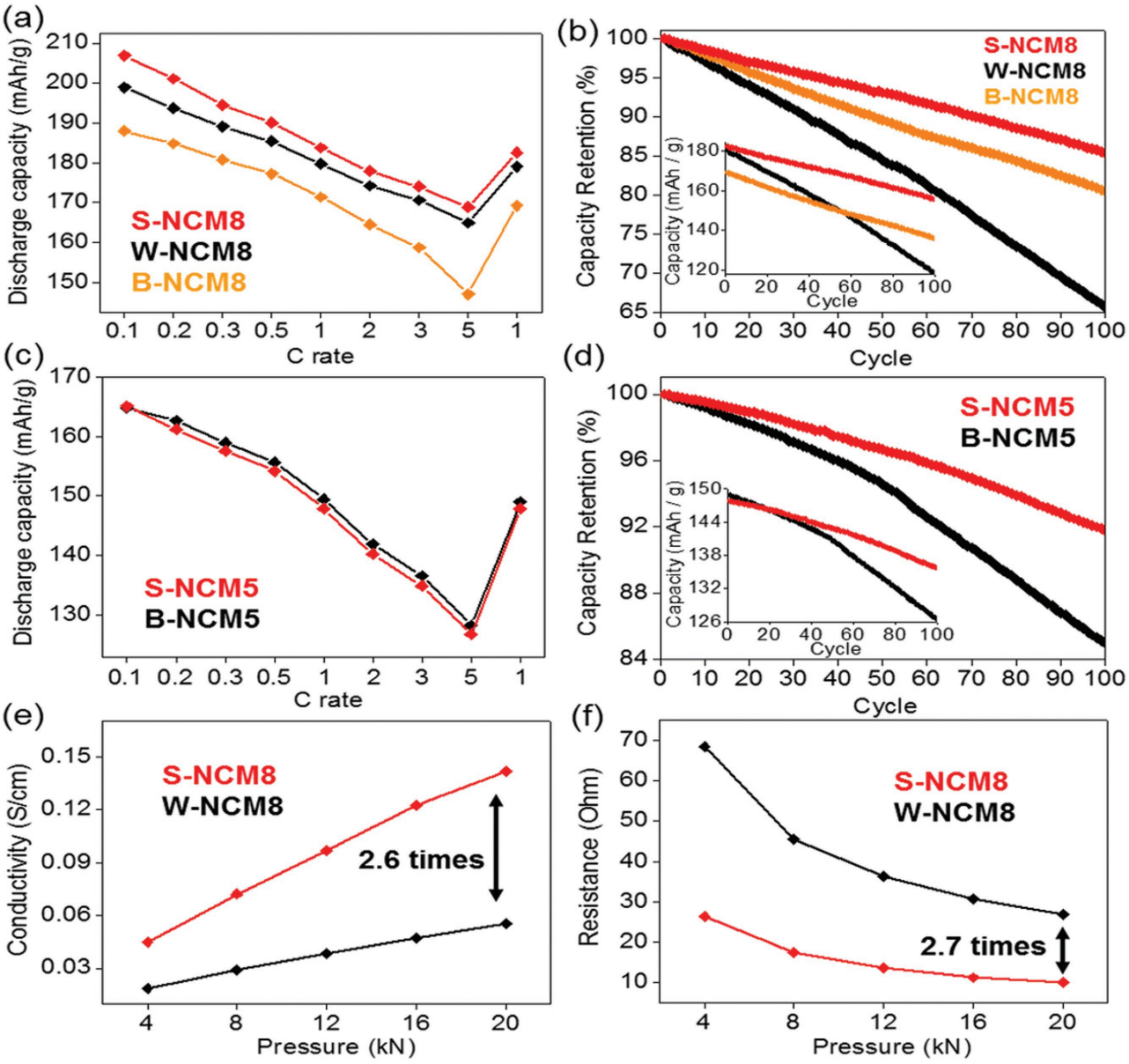

Figure 4. a,b) Galvanostatic discharge capacities (a) and capacity retention (b) of NCM8 and NCM5 at different C-rates, and c,d) cyclic tests over 100 cycles of NCM8 (c) and NCM5 (d). e) Conductivities and f) resistance of S-NCM8 and W-NCM8.

profiling of the NCM materials was performed by Auger electron spectroscopy (AES, Perkin Elmer, SAM 4300). X-ray photoelectron spectroscopy (XPS) was carried out using a Thermo VG and monochromatic Al Kα radiation. The chemical composition of the NCM materials was measured by inductively coupled plasma-mass spectroscopy (ICP-MS, 5300DV, Perkin-Elmer). Electrical properties and electrochemical studies were performed using a powder resistivity measurement system MCP-PD51 and HNT automatic battery cycling system, respectively.

Supporting Information

Supporting Information is available from the Wiley Online Library or from the author.

Acknowledgements

J. Choi and J. Kim contributed equally to this work. This study was supported by 2016 Research Grant from Kangwon National University.

Received: August 11, 2016
Revised: September 15, 2016
Published online: November 9, 2016

[1] a) C. Liu, F. Li, L. P. Ma, H. M. Cheng, *Adv. Mater.* **2010**, *22*, E28; b) F. Cheng, Z. Tao, J. Liang, J. Chen, *Chem. Mater.* **2008**, *20*, 667; c) A. Manthiram, *J. Phys. Chem. Lett.* **2011**, *2*, 176.

[2] a) P. G. Bruce, B. Scrosati, J. M. Tarascon, *Angew. Chem. Int. Ed.* **2008**, *47*, 2930; b) D. Larcher, J. M. Tarascon, *Nat. Chem.* **2015**, *7*, 19.
[3] a) H. J. Yu, H. S. Zhou, *J. Phys. Chem. Lett.* **2013**, *4*, 1268; b) T. Wei, R. Zeng, Y. M. Sun, Y. H. Huang, K. V. Huang, *Chem. Commun.* **2014**, *50*, 1962; c) S. Lee, Y. Cho, H. K. Song, K. T. Lee, J. Cho, *Angew. Chem. Int. Ed.* **2012**, *51*, 8748; d) X. L. Wu, L. Y. Jiang, F. F. Cao, Y. G. Guo, L. J. Wan, *Adv. Mater.* **2009**, *21*, 2710; e) P. Singh, K. Shiva, H. Celio, J. B. Goodenough, *Energ. Environ. Sci.* **2015**, *8*, 3000.
[4] a) Y. K. Sun, Z. H. Chen, H. J. Noh, D. J. Lee, H. G. Jung, Y. Ren, S. Wang, C. S. Yoon, S. T. Myung, K. Amine, *Nat. Mater.* **2012**, *11*, 942; b) M. S. Whittingham, *Chem. Rev.* **2004**, *104*, 4271; c) P. Y. Hou, J. Wang, J. S. Song, D. W. Song, X. X. Shi, X. Q. Wang, L. Q. Zhang, *Chem. Commun.* **2015**, *51*, 3231.
[5] a) D. P. Abraham, R. D. Twesten, M. Balasubramanian, I. Petrov, J. McBreen, K. Amine, *Electrochem. Commun.* **2002**, *4*, 620; b) R. R. Liu, X. Deng, X. R. Liu, H. J. Yan, A. M. Cao, D. Wang, *Chem. Commun.* **2014**, *50*, 15756.
[6] a) Y. Kim, H. S. Kim, S. W. Martin, *Electrochim. Acta.* **2006**, *52*, 1316; b) Y. K. Fan, J. M. Wang, Z. Tang, W. C. He, J. Q. Zhang, *Electrochim. Acta.* **2007**, *52*, 3870; c) J. Z. Kong, C. Ren, G. A. Tai, X. Zhang, A. D. Li, D. Wu, H. Li, F. Zhou, *J. Power Sources* **2014**, *266*, 433; d) J. Cho, T. J. Kim, J. Kim, M. Noh, B. Park, *J. Electrochem. Soc.* **2004**, *151*, A1899; e) S. J. Shi, J. P. Tu, Y. Y. Tang, Y. Q. Zhang, X. Y. Liu, X. L. Wang, C. D. Gu, *J. Power Sources* **2013**, *225*, 338; f) S. H. Ju, I. S. Kang, Y. S. Lee, W. K. Shin, S. Kim, K. Shin, D. W. Kim, *ACS Appl. Mater. Interfaces* **2014**, *6*, 2546; g) H. Q. Li, H. S. Zhou, *Chem. Commun.* **2012**, *48*, 1201.
[7] a) J. H. Cho, J. H. Park, M. H. Lee, H. K. Song, S. Y. Lee, *Energy Environ. Sci.* **2012**, *5*, 7124; b) X. Xiong, Z. Wang, H. Guo, Q. Zhang, X. Li, *J. Mater. Chem. A* **2013**, *1*, 1284; c) Y. Cho, Y.-S. Lee, S.-A. Park, Y. Lee, J. Cho, *Electrochim. Acta* **2010**, *56*, 333; d) W. Cho, S.-M. Kim, J. H. Song, T. Yim, S.-G. Woo, K.-W. Lee, J.-S. Kim, Y.-J. Kim, *J. Power Soruces* **2015**, *282*, 45.
[8] a) Y. Kim, D. Kim, *ACS Appl. Mater. Interfaces* **2012**, *4*, 586; b) Y. Kim, *ACS Appl. Mater. Interfaces* **2012**, *4*, 2329.
[9] A. N. Koo, H. J. Lee, S. E. Kim, J. H. Chang, C. Park, C. Kim, J. H. Park, S. C. Lee, *Chem. Commun.* **2008**, 6570.
[10] Y. Cho, P. Oh, J. Cho, *Nano Lett.* **2013**, *13*, 1145.
[11] N. Andreu, D. Flahaut, R. Dedryvere, M. Minvielle, H. Martinez, D. Gonbeau, *ACS Appl. Mater. Interfaces* **2015**, *7*, 6629.
[12] a) J. Baltrusaitis, D. M. Cwiertny, V. H. Grassian, *Phys. Chem. Chem. Phys.* **2007**, *9*, 5542; b) J. H. Tong, X. G. Han, S. Wang, X. M. Jiang, *Energy Fuels* **2011**, *25*, 4006; c) Z. Yang, Z. Yao, G. F. Li, G. Y. Fang, H. G. Nie, Z. Liu, X. M. Zhou, X. Chen, S. M. Huang, *ACS Nano* **2012**, *6*, 205.
[13] a) N. Imanaka, K. Okamoto, G. Adachi, *Electrochem. Solid State Lett.* **2002**, *5*, E51; b) E. Torijano, R. A. Vargas, B. E. Mellander, *Phys. Status Solidi C* **2007**, *4*, 4225; c) Z. Z. Peng, R. S. Guo, Z. G. Yin, J. Li, *J. Wuhan Univ. Technol.* **2009**, *24*, 269.